Penrose Superradiance in Nonlinear Optics

Maria Chiara Braidotti,[1] Daniele Faccio,[1,2,*] and Ewan M. Wright[2]
[1]School of Physics and Astronomy, University of Glasgow, G12 8QQ Glasgow, United Kingdom
[2]Wyant College of Optical Sciences, University of Arizona, Tucson, Arizona 85721, USA

(Received 11 July 2020; accepted 15 October 2020; published 6 November 2020)

Particles or waves scattered from a rotating black hole can be amplified through the process of Penrose superradiance, although this cannot currently be observed in an astrophysical setting. Here we theoretically show that analog Penrose superradiance arises naturally in the field of nonlinear optics. A loosely focused signal beam can experience gain or amplification as it glances off a strong vortex pump beam in a nonlinear defocusing medium. Amplification occurs only with the generation and trapping of negative norm modes in the core of the pump vortex, as predicted by Penrose. Our results elucidate a new regime of nonlinear optics involving the notion of an ergoregion, providing further insight into the processes and transient dynamics involved in Penrose superradiance.

DOI: 10.1103/PhysRevLett.125.193902

Introduction.—Penrose or rotational superradiance is a process in which waves scattered from a rotating black hole can extract energy at the expense of the black hole rotational energy. In 1969 Penrose predicted this effect noticing that, for an asymptotic observer, particles that fall inside the ergoregion around a rotating Kerr black hole will have negative energy and thus lead to amplification of a reflected positive energy component [1]. This concept was later extended by Zel'dovich to the prediction of amplification of waves reflected from a rotating, metallic (i.e., absorbing) cylinder [2–4], with recent theoretical [5–7] and experimental studies [8] using sound waves.

In the last decades, analog gravity studies have attracted considerable attention revealing the possibility of investigating inaccessible gravitational phenomena in generic rotating geometries and flows by testing them through tabletop experiments. Since the proposal to study analog Hawking radiation in hydrodynamics [9], many different astrophysical phenomena have been proposed: Hawking radiation, boson stars, and superradiance analogs have been investigated in a variety of fields of physics, ranging from nonlinear optics to Bose-Einstein condensates and hydrodynamics [10–20]. In this framework, the first measurement of analog superradiance was reported in a recent study in classical fluid dynamics in the form of over-reflection of waves carrying orbital angular momentum (OAM) scattered from a rotating vortex in a water tank [21]. Several proposals have extended the concept of superradiance to superfluids, providing a generalized framework for superradiant scattering in terms of Bogoliubov excitations [22–25]. A range of studies have focused on superfluids or photon fluids realized with light, i.e., with an optical beam propagating in a medium with a defocusing nonlinearity that mediates the background repulsive photon-photon interaction. This can be tailored so as to reproduce superfluid dynamics and physical phenomena ranging from shock dynamics to analog black holes [26–37].

In this Letter, we show that analog Penrose superradiance arises naturally in the field of nonlinear optics and identifies an unexpected phase-matching mechanism that transforms a weak interaction process into one that exhibits significant amplification dynamics. We consider a geometry in which a weak, loosely focused probe beam carrying OAM copropagates with a strong vortex pump beam onto a nonlinear defocusing medium. Four-wave mixing (FWM) in turn generates an idler mode that can be trapped in the core of the pump vortex via nonlinear cross-phase-modulation. We verify that the conditions for this to occur correspond to the trapped modes having a negative norm, as suggested by Penrose and in which case the reflected signal power can be amplified.

Basic model and equations.—We consider the interaction between a continuous wave monochromatic pump field E_0 with OAM ℓ and a weak probe signal E_s with OAM n as described by the nonlinear Schrödinger equation (NSE) (see Fig. 1 for a conceptual drawing of interaction geometry). This is solved for the total light field $E = E_0 + E_s + E_i$, where E_i is the "idler" field generated by degenerate FWM, with idler OAM $q = 2l - n$. The NSE for the system is given by [38]

$$i\frac{\partial E}{\partial z} + \frac{1}{2k}\nabla_\perp^2 E + k_0 n_2 |E|^2 E = 0, \tag{1}$$

where n_0 is the linear refractive index, $k = 2\pi n_0/\lambda = k_0 n_0$ is the wave number, $\nabla_\perp^2$ is the transverse Laplacian accounting for optical diffraction, and we consider a defocusing medium with nonlinear coefficient $n_2 < 0$. For copropagating fields along the z axis, the total field E may be written in cylindrical coordinates (r, θ, z) as

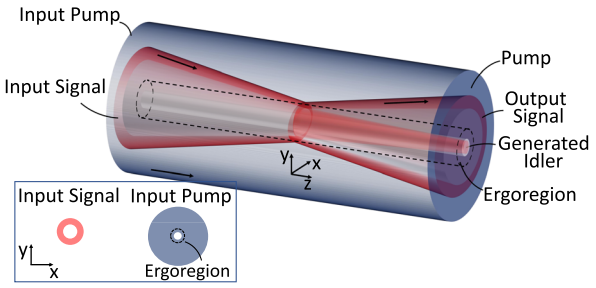

FIG. 1. Conceptual drawing of the interaction geometry. The signal beam is focused on the collimated pump vortex core. Under conditions corresponding to those identified by Penrose, an idler beam is generated that is trapped inside the pump cortex core and the output signal beam is amplified. The inset shows the pump and signal beam transverse profiles at the input (all beams have the same optical frequency).

$$E(r,\theta,z) = E_0 + E_s + E_i = [\mathcal{E}_0(r)e^{i\ell\theta} + \mathcal{E}_s(r,z)e^{in\theta} + \mathcal{E}_i(r,z)e^{iq\theta}]e^{i\beta_\ell z}, \quad (2)$$

where $\beta_\ell = k_0 n_2 I_\ell < 0$, $\mathcal{E}_0(r) = \sqrt{I_\ell}u_\ell(r)$ with I_ℓ as the background intensity of the strong pump vortex with OAM ℓ, and $u_\ell(r)$ as the vortex profile with core size r_ℓ, such that $u_\ell(r) \to 1$ for $r \gg r_\ell$. We employ the approximate vortex profile $u_\ell(r) = \tanh^{|\ell|}(r/W)$ described in Ref. [39]. By substituting Eq. (2) in Eq. (1), linearizing in the signal and idler fields and separating them on the basis of their different OAM, we find

$$\frac{\partial \mathcal{E}_s}{\partial z} = \frac{i}{2k}\nabla_n^2 \mathcal{E}_s + ik_0 n_2[2|\mathcal{E}_0|^2\mathcal{E}_s + \mathcal{E}_0^2\mathcal{E}_i^*] - i\beta_\ell \mathcal{E}_s, \quad (3)$$

$$\frac{\partial \mathcal{E}_i}{\partial z} = \frac{i}{2k}\nabla_q^2 \mathcal{E}_i + ik_0 n_2[2|\mathcal{E}_0|^2\mathcal{E}_i + \mathcal{E}_0^2\mathcal{E}_s^*] - i\beta_\ell \mathcal{E}_i, \quad (4)$$

which describe propagation of the signal and idler fields (see Supplemental Material [40]). Here we have defined $\nabla_p^2 = (\partial^2/\partial r^2) + (1/r)(\partial/\partial r) - (p^2/r^2)$ as the transverse Laplacian for a given OAM p.

We note that, in Eqs. (3) and (4), the longitudinal wave vector shifts for the signal (s) and idler (i) fields $\Delta K_z^{s,i} = k^{s,i} - \beta_\ell$ are referenced to the pump value β_ℓ. Hence, all corresponding effective frequency shifts $\Delta\omega_{s,i} = (\omega_{s,i} - \omega_p) = -c\Delta K_z^{s,i}/n_0$ are with respect to the associated pump frequency $\omega_p = -c\beta_\ell/n_0$ and correspond to phonon frequencies, that is, oscillation frequencies in the transverse plane, analogous to phonons in a 2D fluid [34].

Ergoregion.—We consider two characteristic speeds: the underlying flow speed v and the speed of sound v_s of the photon fluid, i.e., transverse perturbation modes [22,34–36]. The ergoregion is defined as the region in the (x, y) plane where $v > v_s$. In photon fluids, the speed of sound is defined as $v_s = (c/n_0)\sqrt{|\Delta n|/n_0}$, where $\Delta n = n_2 I_\ell$ is the nonlinear change in refractive index due to the pump intensity I_ℓ [34]. The flow speed is $v = |\Omega|r = (c/n_0)(|n-\ell|/kr)$, where Ω is the pump rotational frequency with respect to the perturbation [24]. Equating $v_s = v$ at the ergoradius yields $r_e = (|n-\ell|/k)\sqrt{n_0/|\Delta n|}$.

Positive and negative modes and currents.—Penrose superradiance is based on the concept of positive and negative energy modes: Negative energy modes can remain trapped within the ergoregion, allowing positive energy modes to escape, thereby gaining energy [1,20]. It has been shown [24,32] that Eqs. (3) and (4) exhibit a conserved quantity $N(z)$, also referred to as a Noether current which, in our system, corresponds to $J^0(r,z)$, where $\partial_z J^0 = 0$ and $J_0 = |E_s|^2 - |E_i|^2$, such that

$$N(z) = \int_0^\infty (|E_s|^2 - |E_i|^2) r dr = \text{const.} \quad (5)$$

Negative norm modes arise here from the idler wave intensity $|E_i|^2$. Assuming the signal has unit incident norm, from Eq. (5) we may define the reflection R and transmission T coefficients for the modes scattering from the ergoregion: $R(z) = \int_{r_e}^\infty (|E_s|^2 - |E_i|^2) r dr$ and $T(z) = \int_0^{r_e} (|E_s|^2 - |E_i|^2) r dr$.

Superradiance results in a reflection coefficient larger than 1, such that the reflected field has gained energy (or has been over-reflected) after scattering with the rotating body. The current J_0 is therefore a key signature for establishing the presence of superradiance, which can be identified by the presence of negative current ($J_0 < 0$) inside the scattering region r_e, balanced with a positive current ($J_0 > 0$) outside r_e [24].

A negative current inside r_e will naturally arise if the idler wave becomes trapped inside the ergoregion, while the signal is scattered outward (i.e., the signal and idler beams are spatially separated from each other). In real black holes the trapping can be provided by the event horizon [20].

Trapping of the idler wave.—Neglecting any effect of the idler on the signal propagation to lowest order in Eq. (3), and assuming that the signal beam is not too tightly focused, we take the signal field as a focused Laguerre-Gaussian (LG) beam with radial mode index $p = 0$, OAM n, and focused spot size w_0,

$$\mathcal{E}_s(r,z) \approx c_s V_n(r,z) e^{-i(1+|n|)\phi_G(z)} e^{2i\beta_\ell \Gamma_n(z) z - i\beta_\ell z}, \quad (6)$$

where c_s is the signal field amplitude, $V_n(r,z)$ is the normalized z-dependent LG mode profile. $\Gamma_n(z) = \int_0^\infty 2\pi r dr |V_n(r,z)|^2 u_\ell^2(r)$ describes the variation of the signal phase due to penetration of the LG mode into the pump vortex core. From Eq. (6) we can write the signal wave vector (nonlinear) shift as

$$\Delta K_s \approx \Delta K_s(0) = 2\beta_\ell \Gamma_n(0) - \beta_\ell, \tag{7}$$

where we accounted for the fact that most of the nonlinear interaction will occur within a Rayleigh range around the beam focus at $z = 0$. The overlap factor $0 \le \Gamma_n(0) \le 1$ may be evaluated numerically. At the focus, the radius of the single-ringed LG beam is $r_n = w_0\sqrt{|n|/2}$. Moreover, we require $r_n \approx r_e$ in order for the signal LG ring beam to glance off the ergosphere at it goes through its focus.

We now consider the idler propagation according to Eq. (4). This can be rearranged as

$$\frac{\partial \mathcal{E}_i}{\partial z} = \frac{i}{2k}\nabla_q^2 \mathcal{E}_i + \underbrace{i2\beta_\ell[u_\ell^2(r) - 1]}_{\text{waveguide}}\mathcal{E}_i + i\beta_\ell \mathcal{E}_i + \underbrace{i\beta_\ell u_\ell^2(r)\mathcal{E}_s^*}_{\text{source}}, \tag{8}$$

such that it is composed of two terms: (i) a two-dimensional waveguide term, $2|\beta_\ell|[1 - u_\ell^2(r)] = k_0\Delta n(r)$, that arises from the cross-phase-modulation induced by the pump vortex on the idler wave and, (ii) a source term describing how the idler wave (absent at the input) is driven by the signal beam [40].

It is useful to assess the idler guided modes $U_{pq}(r)$ that arise in the presence of the waveguide term in Eq. (8) while ignoring the source term

$$\mathcal{E}_i(r, z) = c_i(z)U_{pq}(r)e^{i(\beta_\ell + \Lambda_{pq})z}, \tag{9}$$

with $c_i(z)$ as the idler amplitude, radial mode index p, eigenvalue Λ_{pq}, and idler wave vector $\Delta K_i = \beta_\ell + \Lambda_{pq}$. To verify the existence of guided modes, we compute the spectrum of the idler waves with OAM q for a given pump vortex profile $u_\ell(r)$ and value of the nonlinear parameter β_ℓ (see the Supplemental Material [40]). We can then find a condition for the incident signal field to excite a guided idler mode by substituting the guided idler field of the form of Eq. (9) into Eq. (4), with the signal field in Eq. (6), giving

$$\frac{dc_i}{dz} = ic_s^*\beta_\ell F(z)\underbrace{e^{-i[2\Delta K z - (1+|n|)\phi_G(z)]}}, \tag{10}$$

where

$$\Delta K = \left(\frac{\Delta K_s + \Delta K_i}{2}\right),$$
$$F(z) = \int_0^\infty 2\pi r dr V_n^*(r, z)u_\ell^2(r)U_q^*(r), \tag{11}$$

where ΔK is the average wave vector shift of the total perturbation formed by the signal plus idler fields. It is possible to solve Eq. (10) numerically to explore how effectively the signal excites the idler guided mode for a given set of parameters, but the main insight can be gained by looking at phase-matching conditions dictated by the underbraced exponential phase factor. In the vicinity of the origin, the phase factor is approximately $[2\Delta K z - (1 + |n|)z/z_0]$, so that

$$\Delta K = [2\beta_\ell \Gamma_n(0) - \beta_\ell] + (\beta_\ell + \Lambda_q). \tag{12}$$

If the Gouy phase-shift term is zero ($\phi_G = 0$), then $\Delta K = 0$ for phase matching and efficient generation but a more general condition $\Delta K > 0$ guarantees the possibility of phase matching. Indeed, similar phase factors as in Eq. (10) along with the $\Delta K > 0$ condition appear in the theory of harmonic generation using focused beams [38]. In our system, the $\Delta K > 0$ condition can be used to determine whether the guided idler waves can be excited, with consequent observation of Penrose superradiance.

Zel'dovich-Misner condition.—The condition $\Delta K > 0$ can be recast in terms of transverse perturbation (i.e., phonon) frequencies as $\Delta\omega = -(c/n_0)\Delta K < 0$, where $\Delta\omega = [(\Delta\omega_s + \Delta\omega_i)/2]$ is the average of the frequency shifts of the signal and idler fields, with $\Delta\omega_{s,i} = -(c/n_0)\Delta K_{s,i}$. We note that $\Delta\omega = (\omega - \omega_p) = (\omega - m\Omega)$, with $m = (n - \ell)$. So the condition to see Penrose superradiance is $(\omega - m\Omega) < 0$. This has the same form as the Zel'dovich-Misner condition [2,41], therefore establishing the connection between the nonlinear dynamics of the optical beams and the cornerstone relation for Penrose superradiance.

Numerical simulations.—To quantitatively study our proposed nonlinear optics platform for Penrose superradiance, we numerically simulate Eqs. (3) and (4) in a defocusing nonlinear medium. We assume a strong vortex pump beam that does not vary with propagation distance z and neglect absorption. To reveal the generic nature of our results, we employ dimensionless variables with transverse coordinates in units of the signal spot size w, and z is in units of the Rayleigh range $Z_R = kw^2/2$ [42]. Since multiple charge vortices are dynamically unstable due to physics akin to the processes discussed here [43], we consider a pump beam with OAM $\ell = 1$. The background fluid is then generated by a vortex pump, $E_0(r) = \sqrt{I_1}\tanh(r/2)e^{i\theta}$ (based on $W = 2w$). In addition, the input signal with OAM n is taken as a Laguerre-Gaussian beam

$$E_s(r, z = 0) = N_s\left(\frac{r}{w}\right)^{|n|}e^{-(r^2/w^2)}e^{in\theta}, \tag{13}$$

where N_s is a normalization constant, and the idler beam is chosen to have zero amplitude at the input.

Figures 2(a)–2(h) show the signal and idler evolution for two cases. (1) Figures 2(a)–2(d): in this case $\Delta K > 0$ and the signal undergoes superradiant amplification while the idler remains trapped inside the ergoregion. (2) Figures 2(e)–2(h): in this case $\Delta K < 0$ and superradiance

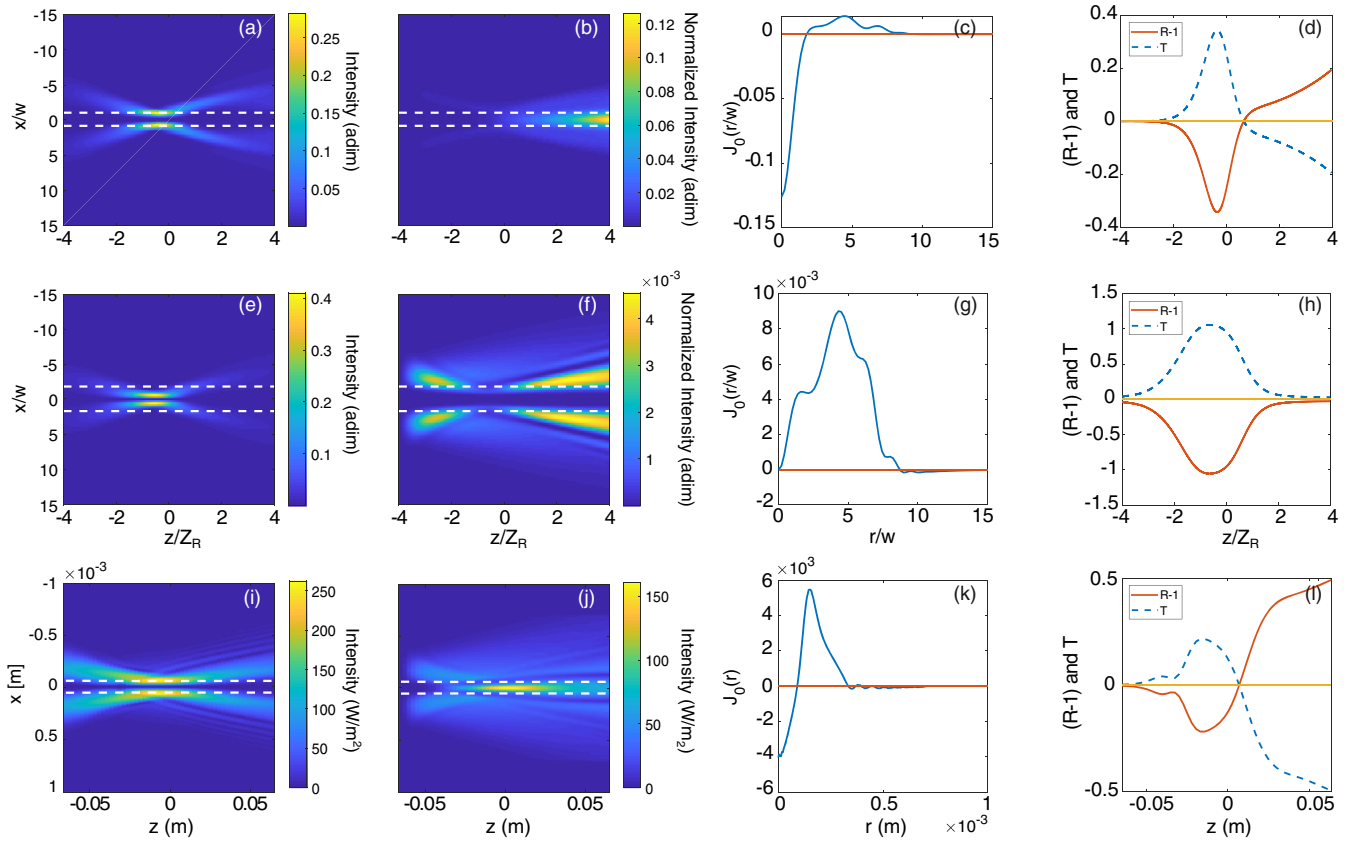

FIG. 2. For all cases, the pump has OAM $\ell = 1$. (a)–(d) For this case, the signal has OAM $n = 2$ and idler OAM $q = 0$, and Penrose superradiance occurs, $\Delta K > 0$. Cross sections for the intensity profiles $|E_{s,i}(x, y, z)|^2$ versus x/w and z/Z_R for $y = 0$ for the (a) signal and (b) idler, calculated using the linearized theory: (c) Current $J_0(r/w)$ versus radius r/w for $z/Z_R = 4$ and (d) reflection $(R - 1)$ and transmission T versus propagation distance z/Z_R. (e)–(h) As in (a)–(d) for signal with OAM $n = -1$ and idler with OAM $q = 3$ for which Penrose superradiance is absent, $\Delta K < 0$. (i)–(l) As in (a)–(d) calculated using the full NSE (1). The horizontal dashed white lines in (a),(b),(e),(f) indicate the location of the dimensionless radius r/w of the ergoregion.

does not occur. The horizontal dashed white lines in Figs. 2(a), 2(b), 2(e), and 2(f) indicate the location of the dimensionless radius r/w of the ergoregion.

In more detail, for Figs. 2(a)–2(d) the signal with OAM $n = 2$ intensity profile $|E_s(x, y = 0, z)|^2$ versus (z/Z_R) is shown in Fig. 2(a) along with the corresponding idler intensity with OAM $q = 0$ in Fig. 2(b). The idler field is initially absent. As the signal diffracts away from the ergoregion for $(z/Z_R) > 0$, it experiences a transient amplification. Conversely, the idler is generated and becomes trapped. In the context of Penrose superradiance, we interpret this as evidence that negative energy waves are trapped during the interaction, while positive energy waves are reflected (no signal inside the ergoregion). This is further confirmed by the plot of the current $J_0(r/w)$ versus r/w at $(z/Z_R) = 4$ in Fig. 2(c). We see that within the ergoregion the current is negative as implied by our theoretical analysis. Figure 2(d) shows the (change in) reflection $(R - 1)$ and transmission (T) coefficients, defined in Eq. (5), indicating an amplification of 19%.

Figures 2(e)–2(h) show the corresponding results for the case with no superradiance, $\Delta K < 0$. Here the signal OAM is $n = -1$ giving OAM $q = 3$ for the idler. The signal [Fig. 2(e)] is no longer amplified and the idler [Fig. 2(f)] is no longer trapped inside the ergoregion. The current [Fig. 2(g)] is now positive near the origin and the reflection coefficient is $(R - 1) \simeq -2\%$ [Fig. 2(h)]; i.e., the signal experiences a small loss (no amplification). These results illustrate that trapping of a negative mode (the idler) inside the ergoregion and amplification of the signal go hand in hand, as expected for Penrose superradiance.

In order to validate the possibility of superradiance in a real photon fluid experiment, we simulate the interaction with the full NSE (1) in a defocusing nonlinear medium. The sample parameters are chosen based on previous experiments in photon fluids experiments with linear refractive index $n_0 = 1.32$ and nonlinear refractive index $n_2 = 1.2 \times 10^{-10}$ m^2/W [34,35,37]. The nonlinearity is assumed to be local as in experiments with Rb atoms [36] or in time-gated measurements in thermal media [37].

The initial field is a beam at wavelength $\lambda = 532$ nm given by the superposition of a pump super-Gaussian vortex $e^{-(r/w_0)^{10}} \tanh^{|\ell|}(r/W) e^{i\ell\theta}$ with $\ell = 1$ and a Laguerre-Gaussian probe signal with $n=2$. The Rayleigh

range for the signal beam is $Z_R \simeq 2$ cm. The pump power is chosen as 140 mW as in [37], with a weak signal beam $P_s = 10^{-2} P_{\text{pump}}$. Figures 2(i)–2(l) in the bottom row show the same quantities as the top row for the chosen parameters, and the results show all of the main features of Penrose superradiance, including a negative current near the origin in Fig. 2(k), trapping of the idler beam in Fig. 2(j), and amplification up to 50% in Fig. 2(l). The relevance of these results is that they no longer rely on the assumption that the pump vortex does not evolve with propagation distance. The amount of amplified reflection is greater for the full simulation as the strict phase-matching condition for a fixed pump is relaxed and allows for a net stronger and spatially extended interaction.

Conclusions.—Optical signal amplification in a nonlinear medium is a well-known process that conserves momentum and also OAM. However, these processes are efficient only in the presence of phase matching that allows accumulation of energy at both signal and idler waves at the expense of the pump beam. Here we have shown an interaction geometry involving beams with OAM that is not phase matched and under normal circumstances leads to a decrease of the input signal power. By making a physical connection between the conditions dictated by Penrose for rotating black holes and the optical case, we were able to identify the interaction conditions that transform the interaction from lossy ($1 - R < 0$) or no amplification to one with amplification up to 50%. The results imply a new amplification regime in nonlinear optics that is tightly connected to the trapping and spatial separation of the idler beam that leads to a transient gain in the signal beam. This bears a close connection to non-normal dynamics in a coupled resonator system in the presence of loss in one of the resonator modes [44]. These results pave the way toward future experiments on superradiant amplification in nonlinear optics and a deeper understanding of the fundamental physics and transient dynamics of Penrose superradiance.

The authors acknowledge financial support from EPSRC (UK Grant No. EP/P006078/2) and the European Union's Horizon 2020 Research and Innovation Programme, Grant Agreement No. 820392.

*Corresponding author.
daniele.faccio@glasgow.ac.uk

[1] R. Penrose, Riv. Nuovo Cimento **1**, 252 (1969) [Gen. Relativ. Gravit. **34**, 1141 (2002)].
[2] Y. B. Zel'dovich, Pis'ma Zh. Eksp. Teor. Fiz. **14**, 270 (1971) [JETP Lett. **14**, 180 (1971)].
[3] C. Gooding, S. Weinfurtner, and W. G. Unruh, Phys. Rev. A **101**, 063819 (2020).
[4] M. C. Braidotti, A. Vinante, G. Gasbarri, D. Faccio, and H. Ulbricht, Phys. Rev. Lett. **125**, 140801 (2020).
[5] C. Gooding, S. Weinfurtner, and W. G. Unruh, arXiv: 1809.08235.
[6] D. Faccio and E. M. Wright, Phys. Rev. Lett. **123**, 044301 (2019).
[7] C. Gooding, Phil. Trans. R. Soc. A **378**, 20200003 (2020).
[8] M. Cromb, G. Gibson, E. Toninelli, M. Padgett, E. Wright, and D. Faccio, Nat. Phys. **16**, 1069 (2020).
[9] W. G. Unruh, Phys. Rev. Lett. **46**, 1351 (1981).
[10] M. Visser, C. Barceló, and S. Liberati, Living Rev. Relativity **8**, 12 (2005).
[11] D. Faccio, F. Belgiorno, S. Cacciatori, V. Gorini, S. Liberati, and U. Moschella, *Analogue Gravity Phenomenology* (Spinger, New York, 2013).
[12] L. J. Garay, J. R. Anglin, J. I. Cirac, and P. Zoller, Phys. Rev. Lett. **85**, 4643 (2000).
[13] L. J. Garay, J. R. Anglin, J. I. Cirac, and P. Zoller, Phys. Rev. A **63**, 023611 (2001).
[14] R. Schützhold, G. Plunien, and G. Soff, Phys. Rev. Lett. **88**, 061101 (2002).
[15] S. Giovanazzi, C. Farrell, T. Kiss, and U. Leonhardt, Phys. Rev. A **70**, 063602 (2004).
[16] I. Zapata, M. Albert, R. Parentani, and F. Sols, New J. Phys. **13**, 063048 (2011).
[17] J. Steinhauer, Nat. Phys. **10**, 864 (2014).
[18] J. Steinhauer, Nat. Phys. **12**, 959 (2016).
[19] F. Belgiorno, S. L. Cacciatori, M. Clerici, V. Gorini, G. Ortenzi, L. Rizzi, E. Rubino, V. G. Sala, and D. Faccio, Phys. Rev. Lett. **105**, 203901 (2010).
[20] R. Brito, V. Cardoso, and P. Pani, *Superradiance* (Springer, New York, 2015).
[21] T. Torres, S. Patrick, A. Coutant, M. Richartz, E. W. Tedford, and S. Weinfurtner, Nat. Phys. **13**, 833 (2017).
[22] F. Marino, Phys. Rev. A **78**, 063804 (2008).
[23] F. Marino, M. Ciszak, and A. Ortolan, Phys. Rev. A **80**, 065802 (2009).
[24] A. Prain, C. Maitland, D. Faccio, and F. Marino, Phys. Rev. D **100**, 024037 (2019).
[25] D. D. Solnyshkov, C. Leblanc, S. V. Koniakhin, O. Bleu, and G. Malpuech, Phys. Rev. B **99**, 214511 (2019).
[26] Y. Pomeau and S. Rica, C. R. Acad. Sci. Paris t. **317**, 1287 (1993).
[27] R. Y. Chiao and J. Boyce, Phys. Rev. A **60**, 4114 (1999).
[28] W. Wan, S. Jia, and J. Fleischer, Nat. Phys. **3**, 46 (2007).
[29] N. Ghofraniha, C. Conti, G. Ruocco, and S. Trillo, Phys. Rev. Lett. **99**, 043903 (2007).
[30] D. Gerace and I. Carusotto, Phys. Rev. B **86**, 144505 (2012).
[31] M. Elazar, V. Fleurov, and S. Bar-Ad, Phys. Rev. A **86**, 063821 (2012).
[32] I. Carusotto, Proc. R. Soc. A **470**, 20140320 (2014).
[33] P.-E. Larré and I. Carusotto, Phys. Rev. A **92**, 043802 (2015).
[34] D. Vocke, T. Roger, F. Marino, E. M. Wright, I. Carusotto, M. Clerici, and D. Faccio, Optica **2**, 484 (2015).
[35] D. Vocke, K.Wilson, F. Marino, I. Carusotto, E. M. Wright, T. Roger, B. P. Anderson, P. Ohberg, and D. Faccio, Phys. Rev. A **94**, 013849 (2016).
[36] Q. Fontaine, T. Bienaimé, S. Pigeon, E. Giacobino, A. Bramati, and Q. Glorieux, Phys. Rev. Lett. **121**, 183604 (2018).
[37] D. Vocke, C. Maitland, A. Prain, F. Biancalana, F. Marino, E. M. Wright, and D. Faccio, Optica **5**, 1099 (2018).

[38] R. W. Boyd, *Nonlinear Optics*, 2nd ed. (Academic Press, New York, 2002).
[39] I. Velchev, A. Dreischuh, D. Neshev, and S. Dinev, Opt. Commun. **140**, 77 (1997).
[40] See Supplemental Material at http://link.aps.org/supplemental/10.1103/PhysRevLett.125.193902 for details on the derivation of equations.
[41] C. W. Misner, Phys. Rev. Lett. **28**, 994 (1972).
[42] G. R. Fowles, *Introduction to Modern Optics*, 2nd ed. (Dover Publications, Inc., New York, 1989).
[43] L. Giacomelli and I. Carusotto, Phys. Rev. Research **2**, 033139 (2020).
[44] D. Politzer, Am. J. Phys. **83**, 395 (2015).